Developmental Biology 451 (2019) 79–85

Contents lists available at ScienceDirect

Developmental Biology

journal homepage: www.elsevier.com/locate/developmentalbiology

The regulation of cell size and branch complexity in the terminal cells of the *Drosophila* tracheal system

Alondra Schweizer Burguete[a,1], Deanne Francis[c,2], Jeffrey Rosa[d,3], Amin Ghabrial[b,*,1]

[a] The Taub Institute, Columbia University Medical Center, New York, NY 10032, USA
[b] Department of Pathology and Cell Biology, Columbia University Medical Center, 630 168th St, New York, NY 10032, USA
[c] Charles Perkins Centre, The University of Sydney, Sydney, Australia
[d] MCDB Department, UCLA, BSRB 450B 621 Charles E. Young Drive S., Los Angeles, CA 90095-1606, USA

ABSTRACT

The terminal cells of the larval *Drosophila* tracheal system extend dozens of branched cellular processes, most of which become hollow intracellular tubes that support gas exchange with internal tissues. Previously, we undertook a forward genetic mosaic screen to uncover the pathways regulating terminal cell size, morphogenesis, and the generation and maintenance of new intracellular tubes. Our initial work identified several mutations affecting terminal cell size and branch number, and suggested that branch complexity and cell size are typically coupled but could be genetically separated. To deepen our understanding of these processes, we have further characterized and determined the molecular identities of mutations in the genes *sprout, denuded* and *asthmatic,* that had been implicated in our initial screen. Here we reveal the molecular identity of these genes and describe their function in the context of the TOR and Hippo pathways, which are widely appreciated to be key regulators of cell and organ size.

1. Introduction

Over the course of normal development in the *Drosophila* trachea, increases in organ size correlate with increases in branch number. In prior work, we determined that mutations that affect cell size tend to have a corresponding effect on branch number (Ghabrial et al., 2011). Nearly all larval tracheal cells are post-mitotic, hence, the dramatic increase in organ size and number of tracheal tubes from embryonic stages to the end of the third larval instar must be mediated almost exclusively through pathways that regulate cell size. Among these are the target of Rapamycin (TOR) and Hippo pathways (Tumaneng et al., 2012a). Increased signaling through the Hippo and TOR pathways, as seen when their respective inhibitors, Warts and TSC1, are removed, result in increased terminal cell size and ectopic branching (Ghabrial et al., 2011). The Hippo pathway acts principally through controlling the subcellular localization of transcriptional factor Yorkie/YAP (Johnson and Halder, 2014; Tumaneng et al., 2012b). The TOR pathway integrates Insulin signaling and other nutritional information, such as amino acid availability, to promote growth and proliferation through increased rates of protein synthesis (Edgar, 2006; Hietakangas and Cohen, 2009). Both Hippo and TOR pathways also regulate DNA replication and ploidy (Jiang et al., 2014; Pierce et al., 2004; Zielke et al., 2011). For both pathways, downstream effectors remain to be fully elucidated.

In post-mitotic tissues, endoreplication is a commonly used strategy to promote growth, with DNA replication controlled by genes downstream of TOR and Hippo pathways (Zhang et al., 2000). For example, both pathways have been shown to regulate the transcription factor, E2F1, which initiates S-phase by transcribing *Cyclin E* (Bayarmagnai et al., 2012; Duronio and O'Farrell, 1995; Duronio et al., 1995; Reddy et al., 2010; Zhang et al., 2017). Endoreplication occurs in most larval cells during the 5 days of growth leading up to pupariation. Many cells in the tracheal system have been shown to endoreplicate (Guha and Kornberg, 2005; Zhou et al., 2016), while a pool of undifferentiated tracheoblasts remain diploid and are activated to divide and populate much of the pupal and adult tracheal system during the third larval instar (Guha and Kornberg, 2005; Weaver and Krasnow, 2008). However, some differentiated tracheal cells that contribute to smaller tubes, such as the anterior dorsal branch stalk cells, maintain their mitotic potential, as do a small subset of cells (tr2)

* Corresponding author.
E-mail addresses: asb2272@cumc.columbia.edu (A.S. Burguete), asg2236@cumc.columbia.edu (A. Ghabrial).
[1] Co-Senior Authors.
[2] Present address.
[3] Present address.

https://doi.org/10.1016/j.ydbio.2019.02.001
Received 5 September 2018; Received in revised form 28 January 2019; Accepted 4 February 2019
Available online 05 February 2019
0012-1606/

in the larger dorsal trunk tubes. During larval stages, these differentiated cells enter S-phase, label with phospho-histone H3 antibody, alter their morphology, and proliferate, ultimately contributing multiple cell types to the pupal tracheal system (Weaver and Krasnow, 2008). Tracheal terminal cells do not contribute to the pupal tracheal system; however, whether they endoreplicate and if that is important for cell size and branch complexity has not been explicitly addressed.

In addition to examining known regulators of cell size, we have continued to follow-up on our unbiased genetic approach towards identifying novel factors, some of which could be specific to the tracheal system. Previously, we found that mutations in essential house-keeping genes, which result in clone loss in mitotic tissues such as the eye imaginal disc, appear to be better tolerated in post-mitotic cells, perhaps due to perdurance of mRNA and/or protein present in the mother cell. For example, while eye imaginal disc clones mutant for glutamyl-prolyl tRNA synthetase are lost or restricted to a few cells in size, tracheal cells mutant for glutamyl-prolyl-tRNA synthetase were recovered at a relatively high frequency but found to decrease both cell size and branch number (Ghabrial et al., 2011). Mutations in other genes likewise had a strong effect on terminal cell size and branch number including mutations in the tracheal master transcription factor, *trachealess* (*trh*), and the terminal cell-specific transcription factor *blistered*/SRF (Ghabrial et al., 2011; Guillemin et al., 1996).

On the other hand, mutations in tumor suppressor genes, which cause dramatic over-proliferation defects in eye clones, were recovered as mutant tracheal terminal cells with abnormally large cell bodies and higher numbers of branches (Ghabrial et al., 2011). Such mutants included the Hippo pathway member *warts*/*lats1* (*miracle-gro*), and the TOR pathway inhibitor, *Tsc1* (*jolly green giant*). Consistent with this trend, activation of the FGF Receptor (Breathless) pathway in terminal cells, which results in an increase in cell size, also gives rise to ectopic branches (Jarecki et al., 1999; Lee et al., 1996). Expression of a forced FGFR dimer (λ-*breathless*) resulted in a *warts*-like phenotype, with increased tube diameter, tortuosity, and the generation of tubes coursing through the cell soma (Schottenfeld-Roames and Ghabrial, 2012). It is striking that ectopic branches arise around the terminal cell nucleus, perhaps reflecting that the elevated growth signal lacks a specific spatial cue such as might be provided by a hypoxic tissue secreting the FGFR ligand, Branchless.

Here we examine endoreplication specifically in tracheal terminal cells, determining that they do endoreplicate, primarily during the second larval instar, and that this correlates with increases in cell size and branch complexity. We test a requirement for E2f1, which is essential for endoreplication, in terminal cell growth and branching, and then go on to determine the molecular identities of *sprout*, *denuded* and *asthmatic*, and to characterize the cell size and branch complexity defects of null mutations in those genes. Our data appear to converge on the central role of the Hippo and TOR pathways in the regulation of cell size and branch complexity in tracheal terminal cells.

2. Materials and methods

2.1. Fly strains and mosaic analysis

Mutations in *sprout*, *denuded* and *asthmatic* were previously described in (Ghabrial et al., 2011). FRT82B *E2F* ^{rM729} was from the Bloomington stock center. For mosaic analysis, males carrying the mutation of interest were crossed to virgins of the following genotype: y, w, hsFLP^{122}; btl-GAL4, UAS-GFP, DsRED2^{nls}; FRT82B *cu*, GFP RNAi. For Grim and Hid mis-expression experiments, a classic MARCM approach was used; briefly, males carrying UAS-Grim or UAS-Hid and FRT82B *Tub*-Gal80 were crossed to virgins of the genotype y, w, hsFLP122; *btl*-GAL4, UAS-GFP; FRT2A,FRT82B. For both mosaic strategies, eggs were collected for 4 h and then embryos were subjected to a 1 h heat shock at 38.5 °C. Crosses were maintained at 25 °C. On day 5, wandering third instar larvae were collected for study. For visualization of gross terminal cell morphology and gas filling, larvae were heat killed (5 – 10 s at 70 °C), mounted in glycerol and imaged. For antibody staining, larvae were filleted in ice-cold PBS supplemented with Tween20 and TritonX100 (PBSTw,Tr) and fixed for 15 – 20 min in 4% formaldehyde.

2.2. Immunofluorescence

Fixed fillets were rinsed 3x in PBSTw,Tr (0.3%, 0.3%) and then incubated with primary antibody in PBSTw,Tr supplemented with 4% horse serum overnight at 4 °C. Fillets were then rinsed 3x in PBSTw,Tr (0.3%, 0.3%) and washed 3 × 30 min. Fillets were incubated with secondary antibody in PBSTw,Tr for 2 h at room temperature, and then were rinsed 3x in PBSTw,Tr (0.3%, 0.3%) and washed 3 × 30 min. Larvae were mounted in aquapolymount and imaged on Leica compound fluorescent microscopes. Images were deconvolved using the Leica 3D deconvolution software.

2.2.1. Antibodies

Mouse α-Armadillo (DSHB, AB_528089); chicken α-GFP (Invitrogen, AB_2534023); Rabbit α-PKC-zeta (Santa Cruz, sc-216); Rabbit α-Wkdpep (Ghabrial lab, AB_2737402). Secondary antibodies (Invitrogen) were conjugated to Alexa dyes (A488, A594, or A647) and used at 1:1000 dilutions.

2.2.2. Edu labeling

0.1 mM Edu was mixed with standard fly food, accompanied by a few pellets of bromophenol blue. Larvae sorted under the dissecting microscope based on size and spiracles and transferred to Edu food. Late wandering 3rd instar larvae that ingested bromophenol blue were collected 24–48 h later. Larvae were filleted and Edu was developed according to the Click-it Edu labeling kit followed by standard immunostaining (Invitrogen, C-10419).

2.2.3. Sholl analysis

2nd, early 3rd and late 3rd instar *btl*-GAL4, UAS-GFP; FRT ^{2A},FRT^{82B} larvae were identified based on size and spiracle morphology. Larvae were heat killed and z-stacks of intact terminal cells from the 5th metamere were imaged on the Leica DMR microscope. Terminal cells were processed using the Simple Neurite tracer and the Sholl analysis plug-in using Fiji/imageJ software. Statistical significance was determined was by *t*-Test.

3. Results and discussion

3.1. Tracheal terminal cells endoreplicate

To test whether terminal cells undergo endoreplication, we fed 2nd and early 3rd instar larvae food laced with Edu, (5-ethynyl-2´-deoxyuridine) a nucleoside analog to thymidine, and then examined Edu staining at late third larval instar. While larvae fed at 2nd instar incorporated Edu throughout the trachea including terminal cells (Fig. 1 A-B', n = 7 larvae), and also other tissues, larvae fed at early 3rd instar lacked terminal cell labeling (Fig. 1 C-C', n = 3 larvae). Indeed, with the exception of occasional fusion cells and of cycling tracheoblasts (data not shown), no tracheal Edu incorporation occurred during the third larval instar. As an internal control, we note that Edu labeling was observed in muscle (Fig. 1 D-D'), as well as all other larval tissue examined in larval fillets (data not shown). These data indicate that tracheal DNA replication in larvae mostly occurs prior to 3rd instar. Mutations in genes essential for endoreplication, such as *e2f1*, considered in more detail below, affect nuclear size of third instar terminal cells (Fig. 1E-F'), as expected.

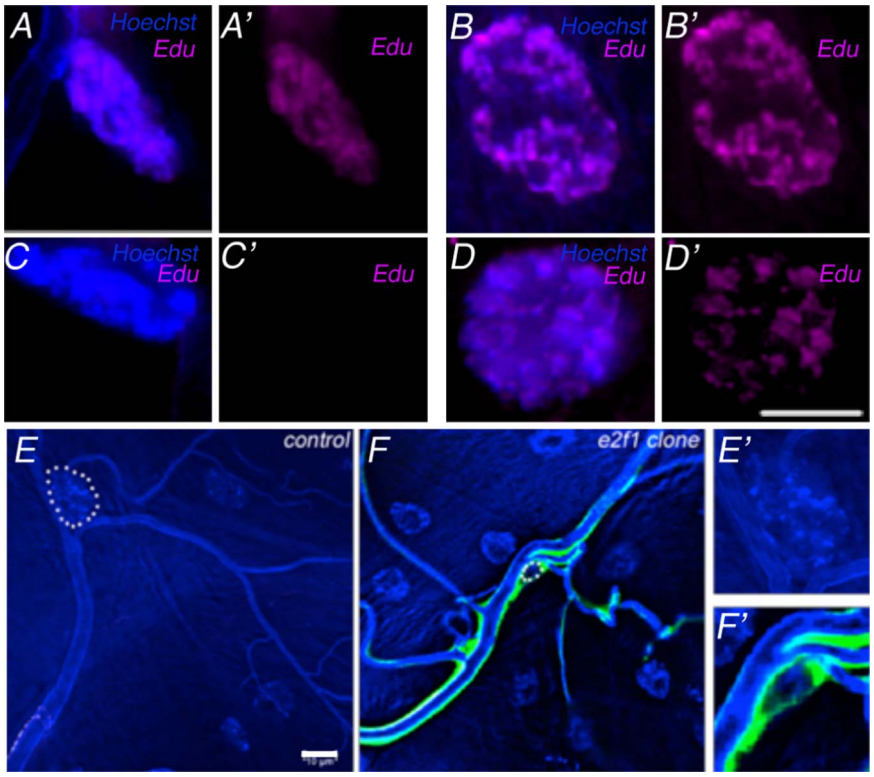

Fig. 1. Endoreplication of Tracheal Terminal Cells. Terminal cells (A, C) and muscle cells (B, D) whose nuclei were visualized by Hoechst staining (blue), were examined for incorporation of Edu (magenta) subsequent to feeding during 2nd (A,B) or early 3rd (C,D) larval instars. All larvae were scored at third wandering instar regardless of the time of feeding. Merged images are shown in A-D, Edu staining only is displayed in A'-D'). Nuclear size is dependent on endoreplication, as cells mutant for e2f1 show dramatically smaller nuclei (compare E, F). In mosaic larvae stained with Hoechst, control terminal cell nuclei (E) were much larger than e2f1 clones marked by GFP expression (F). Terminal cell nuclei are outlined in white dashed circles. Autofluorescence in the UV channel also mark the tubes of the tracheal system. (E') and (F') show enlarged nuclei from (E) and (F), respectively. Scale bars = 10 μm.

3.2. Terminal cell branch complexity increases dramatically between 2nd and 3rd instar

We performed a careful analysis of terminal cell growth during second and third larval instars. Significant increases in branch complexity, quantified as the number of branch intersections at any given distance from the center of the cell (using Sholl analysis as described previously (Schottenfeld-Roames et al., 2014)), was seen between 2nd and early 3rd instar (Fig. 2). Cells continued to extend new branches, and to cover larger areas, during the third instar, but without a similar jump in complexity as seen between 2nd and early 3rd instars. Larvae scored during the second instar had between 3 and 8 branch tips (mean of 4.9), which by early third instar had increased to between 10 and 17 branch tips (mean of 13.3), and by the end of third instar to 18–31 branch tips (mean of 25.1), numbers largely in agreement with those previously reported by JayaNandanan and colleagues (JayaNandanan et al., 2014).

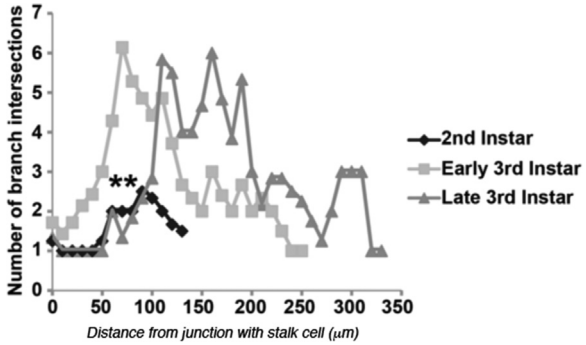

Fig. 2. Branch complexity increases dramatically between 2nd and early 3rd instar. A Sholl analysis of branching complexity was performed at 2nd, early 3rd, and late 3rd instar. In all cases, terminal cells from the 5th tracheal metamere were examined (tr5). The distance from the stalk cell junction at which the circles intersect terminal cell branches are indicated on the X-axis while the number of branches crossed by the circles are indicated on the Y-axis. ** indicates a *T*-Test value of $p < 0.01$ for the comparison of 2nd instar data with that of early and of late 3rd instar, with 7, 7 and 6 terminal cells scored for each stage, respectively.

To test whether endoreplication is required for normal terminal cell growth and branching, we examined cells mutant for the transcription factor E2f1, which is known to be required for S phase during endoreplication in post-mitotic tissues (Orr-Weaver, 2015). Terminal cells mutant for *E2f1* had fewer branches and also showed gas-filling defects (Fig. 3A-B, 100% penetrant phenotype, n = 52, and data not shown). The number of branches per terminal cell ranged from 8 to 18 with a mean of 12 + /- 1 SEM (n = 9). Moreover, we found that the smaller *E2f1* mutant terminal cells induced neighboring wild type stalk cells to increase in size and to invade the small mutant terminal cells (Fig. 3C), much as we had previously observed for mutations in the TOR pathway (Francis and Ghabrial, 2015). Compensatory stalk cell branching, as described in Francis and Ghabrial, results in an increase in stalk cell size and branch complexity, as the stalk cell extends into the terminal cell, much like fingers pushing into a balloon. When this occurs, an increase in the number of intercellular connections between the stalk cell and the terminal cell are observed: in wild type, there is almost always a single intercellular junction connecting the terminal and stalk cell; in the case of compensatory branching, there may be two intercellular junctions (a "mild" phenotype) or more (a "severe" phenotype). Taken together, these data suggest that endoreplication is an important driver of terminal cell growth and branching.

sprout encodes the Drosophila InR. We next turned to mutations in *sprout*, which caused a similar decrease in cell size, but did not appear

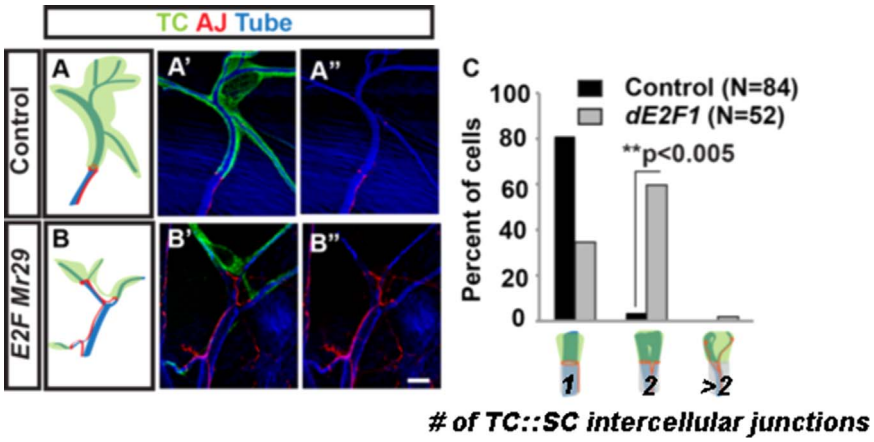

Fig. 3. E2f1 is required for normal terminal cell growth and branching. Terminal cell clones were positively labeled by GFP expression (green) while tracheal tubes were visualized by autofluorescence in the UV channel (blue), and cell junctions were marked by staining against adherens junction (AJ) components (Arm, red). In control terminal cells (A-A"), a ring of AJ staining marks a single intercellular junction with a neighboring (unlabeled) autocellular stalk cell. In E2f1 mutant cells (B-B"), smaller and less branched terminal cells were connected to single stalk cells by two or more cell junctions 61% (n = 28) of the time (C). Data are representative of marked homozygous mutant tracheal terminal cells examined in multiple animals from three replicate crosses to generate genetic mosaic animals. Scale bar = 10 μm.

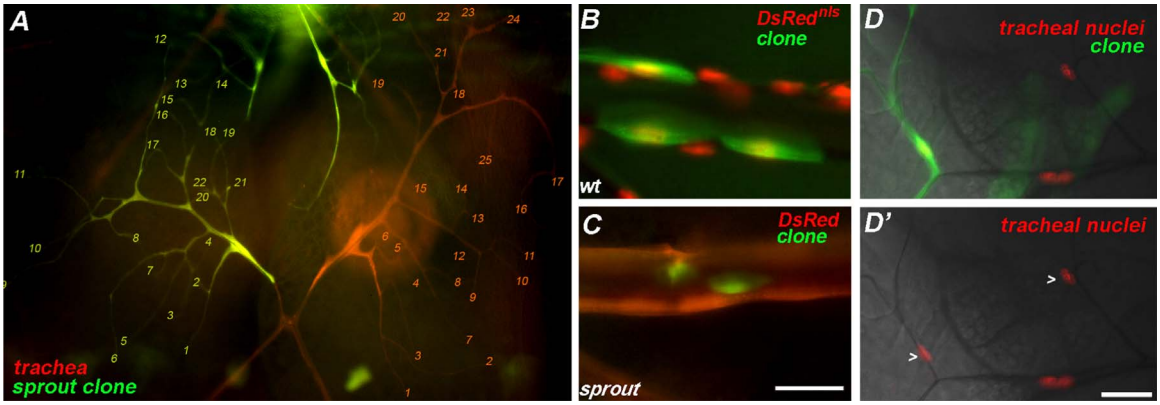

Fig. 4. Terminal cells mutant for *sprout* are reduced in size but not branch complexity. A) A mosaic larva with a *sprout* terminal cell clone (green) is shown; the branch tips for the *sprout* mutant and contralateral control terminal cell are enumerated (21 and 25, respectively). In B-C), control and *sprout* clones, respectively, in the dorsal trunk are shown. Note that in A and C, DsRed counterstains all tracheal cells, while in B and D $DsRed^{nls}$ is employed in the same capacity. In D and D' compare the similar size of *sprout* and heterozygous control terminal cell nuclei (> points to terminal cell nuclei); this is in contrast to staining in terminal cells where endoreplication is blocked. Scale bars = 50 μm. Bar for A, B and C, shown in C, for D and D; shown in D'.

to strongly affect branch number. For instance, the number of branch tips for a *sprout* mutant dorsal branch terminal cell and the control dorsal branch terminal cell on the contralateral side were roughly the same (Fig. 4; 22 +/- 2.3 SEM and 25 +/- 1.9 SEM, respectively; n = 7 *sprout* terminal cells and 7 control terminal cells, which were representative of dozens of terminal cell clones examined in larvae from more than 4 replicate crosses) despite the smaller size of the *sprout* cells. Terminal cells mutant for *sprout* were estimated to have a soma of about 2/3 the size of neighboring terminal cells and to likewise ramify on a target area of about 2/3 the size (n = 5 *sprout* terminal cells, 5 control terminal cells which were representative of the dozens of terminal cell clones examined from more than 3 replicate crosses). In the same mosaic animals, dorsal trunk cells, which were easier to measure due to their simpler hexagonal shapes, *sprout* cells covered areas of ~ ¼ the size of control dorsal trunk cells (n = 3 *sprout*, 5 control dorsal trunk cells). We also note that *sprout* mutant dorsal trunk cells tended to be oval in shape rather than hexagonal.

To gain insight into how *sprout* regulates terminal cell size and branching, we decided to determine the molecular nature of the gene. The mutation in *sprout* mapped distal to FRT82B, and whole genome sequencing identified a nonsense mutation in the *Drosophila Insulin-like Receptor* (Fernandez-Almonacid and Rosen, 1987) (*InR*; Fig. 5A). The *sprout* allele of *InR* is likely a null, as the mutation is predicted to truncate the receptor within the active site of the kinase domain (W1562Stop). Because InR activation antagonizes PTEN (Oldham et al., 2002), which in turn acts as an upstream inhibitor in the TOR pathway we speculate that the decrease in *sprout* cell size is due to decreased TOR signaling. Interestingly, prior work (Dekanty et al., 2005) identified a role of InR, mediated by signaling through the TOR pathway, in modulating Sima protein levels. Sima is the *Drosophila* Hifα ortholog, which regulates terminal cell branching in response to oxygen (Bacon et al., 1998; Centanin et al., 2008). Loss of *InR* is thus predicted to result in decreased Hifα in the nucleus, and might have been expected to lead to even greater reductions in terminal cell branching given that Sima positively regulates the Breathless-FGFR. Why mutations in *InR* do not appear to strongly affect branch complexity remains a question for future study, but may reflect that Sima/Hifα exerts a negative feedback on TOR activity – Hifα-target gene, *Scylla*, activates TSC1-TSC2 (Dekanty et al., 2005) – and additionally, that loss of InR does not impact endoreplication. Indeed, we find no detectable effect on nuclear size or DNA content in *sprout* terminal cell clones as compared to neighboring heterozygous terminal cells in the same animal (Fig. 4D). The lack of effect on endoreplication may also account for the limited ability of mutant *InR* terminal cells to induce compensatory branching of neighboring stalk cells (73% of *sprout*/*InR* terminal cells shared a single intercellular junction with the neighboring stalk cell, while 27% had shared two intercellular junctions, which was elevated from the 4% occurrence observed in wild type).

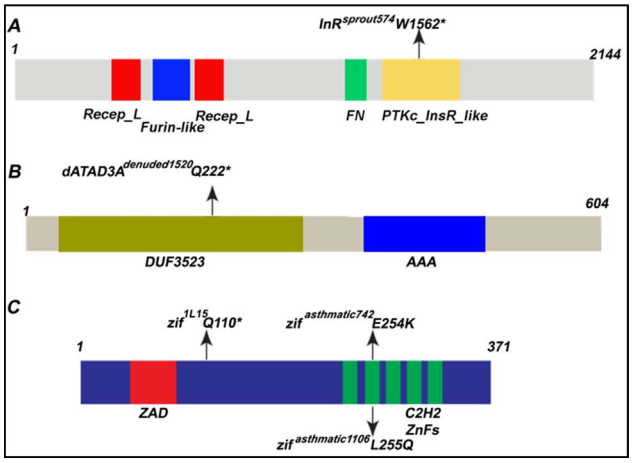

Fig. 5. The molecular identities of *sprout*, *denuded* and *asthmatic*. A) Mapping and whole genome sequencing revealed a nonsense mutation within the coding sequence of InR in *sprout* mutant animals. The mutation is predicted to cause a truncation of the protein within the kinase domain and is therefore likely to be an amorphic allele. B) Mapping and whole genome sequencing of mutations in denuded revealed a nonsense mutation within the coding sequence of dATAD3A. The mutation is predicted to truncate the protein after 222 amino acids, completely deleting the AAA domain. C) Mutations previously assigned to the *asthmatic* complementation group were mapped by meiotic recombination and failed to complement mutations in *zif*. Sequencing of *zif* revealed missense mutations in the second zinc finger domain of the two of the mutations in the *asthmatic* complementation group – see details below. For further analysis of zif/asthmatic, we used the putative null allele, 1L15, that was previously shown to carry a non-sense mutation predicted to truncate the protein such that all zinc finger domains would be lacking.

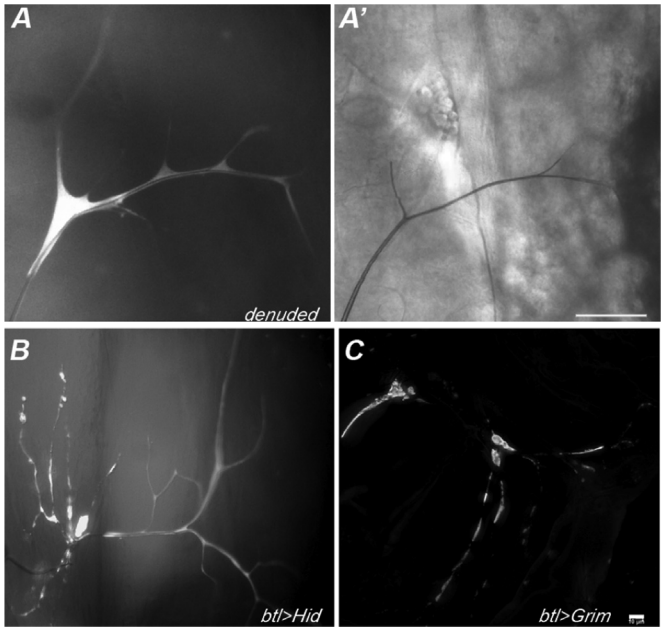

Fig. 6. Terminal cells mutant for *denuded* show reduced size and branch complexity. In mosaic larvae, terminal cells homozygous for *denuded* (*15–20* allele shown) have reduced cell size and branch number. Terminal cell clones were identified as GFP (white) positive cells. In particular, while one or two main branches appear of normal size and gas-filled (A'), side branches are reduced in number and appear thin and whispy. The defects observed in *denuded* clones are not due to apoptosis, as terminal cells induced to apoptose by expression of Hid (B) or Grim (C), using the MARCM system, show blebbing of the cytoplasm and branch loss. Note that extensive branching occurs in these terminal cells prior to the onset of branch loss, this may reflect the delay in GAL4-induced expression associated with turn-over of GAL80 subsequent to clone induction. Scale bar in A' = 50 μm, Scale bar for B,C (in C) = 10 μm.

denuded encodes the Drosophila ATAD3. Tracheal terminal cells mutant for *denuded* frequently formed primary terminal cell branches with seamless tubes of normal morphology, but subsequent generations of branches were pruned or altogether absent (Fig. 6). Through a combination of meiotic recombination mapping and whole genome sequencing, we determined that the *denuded* mutations (Fig. 5B) were in the previously identified gene *belphegor (bor)*/dATAD3A (Harel et al., 2016). ATAD3A is a nuclear-encoded mitochondrial membrane protein that is a downstream effector of TOR – indeed, *bor* was identified as one of the genes most sensitive to rapamycin treatment. ATAD3A and is required for mitochondrial biogenesis and for ER-Mitochondrial interaction (Baudier, 2018; Guertin et al., 2006). Consistent with a role downstream of Tor, we find that terminal cells mutant for *denuded* induced compensatory stalk cell branching (57% of terminal cells shared a single intercellular junction with the adjacent stalk cell, while 41% displayed a mild phenotype with two intercellular junctions and 2% displayed severe defects, with more than 2 intercellular junctions; n = 51). Loss of function in the human *ATAD3A* is implicated in developmental defects and neurological syndromes, such as hereditary spastic paraplegia.

One of our *denuded* alleles (*denuded*^{1520}) is likely to be a molecular null as we determined that a nonsense mutation is present, converting Q222 into a stop codon. The pruning defect is likely to be one associated with reduced growth rather than cell death, since forced expression of pro-apoptic genes in tracheal terminal cells results in dramatic blebbing of the cell, loss of gas-filling, and degeneration of existing branches (Fig. 6 B,C, and data not shown).

3.3. The transcription factor Zif is required for maintenance of apical membrane polarity

Mutations in *asthmatic* were initially identified based on their gas-filling defects – terminal cells and autocellular tubes were affected (Fig. 7). Further analysis showed that the tubes formed by *asthmatic* mutant terminal cells were frequently discontinuous and that the number of side branches were reduced as compared to internal controls. Mapping, complementation tests, and sequence analysis determined that two of the three *asthmatic* mutations are allelic to *zinc finger protein* (*zif*) (Fig. 5C). The third allele of *asthmatic*, *1530*, complemented *zif* and was subsequently found to complement *742* (but not *1106*). Accordingly, we rename the *1106* and *742* mutations as *zif* alleles, and retain the name *asthmatic* for *1530*; whether *1106* also carries a mutation in *asthmatic*, or if *1106* and *1530* carry mutations in a third essential gene has not yet been determined.

Intriguingly, *zif* was previously characterized based on its role in the regulation of the apical domain of neurons, with Zif shown to repress expression of aPKC (Chang et al., 2010). We examined the putative null allele of *zif* (1L15) and found that it showed a more extreme terminal cell phenotype than *742* or *1106*, which carry point mutations in the second zinc finger. Terminal cells null for *zif* were reduced in size, showed little or no branching, and formed discontinuous tubes. Strikingly, the *zif* null terminal cells also showed apical protein localization defects, with aPKC, as well as another apical marker (anti-Wkdpep, (Schottenfeld-Roames and Ghabrial, 2012)), distributed throughout the cell and no longer enriched on the lumenal membrane. The mislocalization of apical proteins was reminiscent of the defects we reported for TOR pathway and vATPase mutants (Francis and Ghabrial, 2015); consistent with that, we observed induction of stalk cell compensatory branching associated with *zif* mutant terminal cells (data not shown). Pan-tracheal RNAi of *zif* resulted in developmental arrest, with only a few unusually small larvae progressing to third instar, and none to pupal stages. Terminal cells were not gas-filled, and other branches were subject to liquid filling under stress. Terminal cells appeared to undergo apoptosis as judged by blebbing of their cytoplasm (similar to the cells shown in Fig. 6B,C, data not shown). Taken together, these data suggest that Zif is required for terminal cells to maintain apical polarity. Interestingly, this requirement in the tracheal system was specific for terminal cells as *zif* clones in other positions in

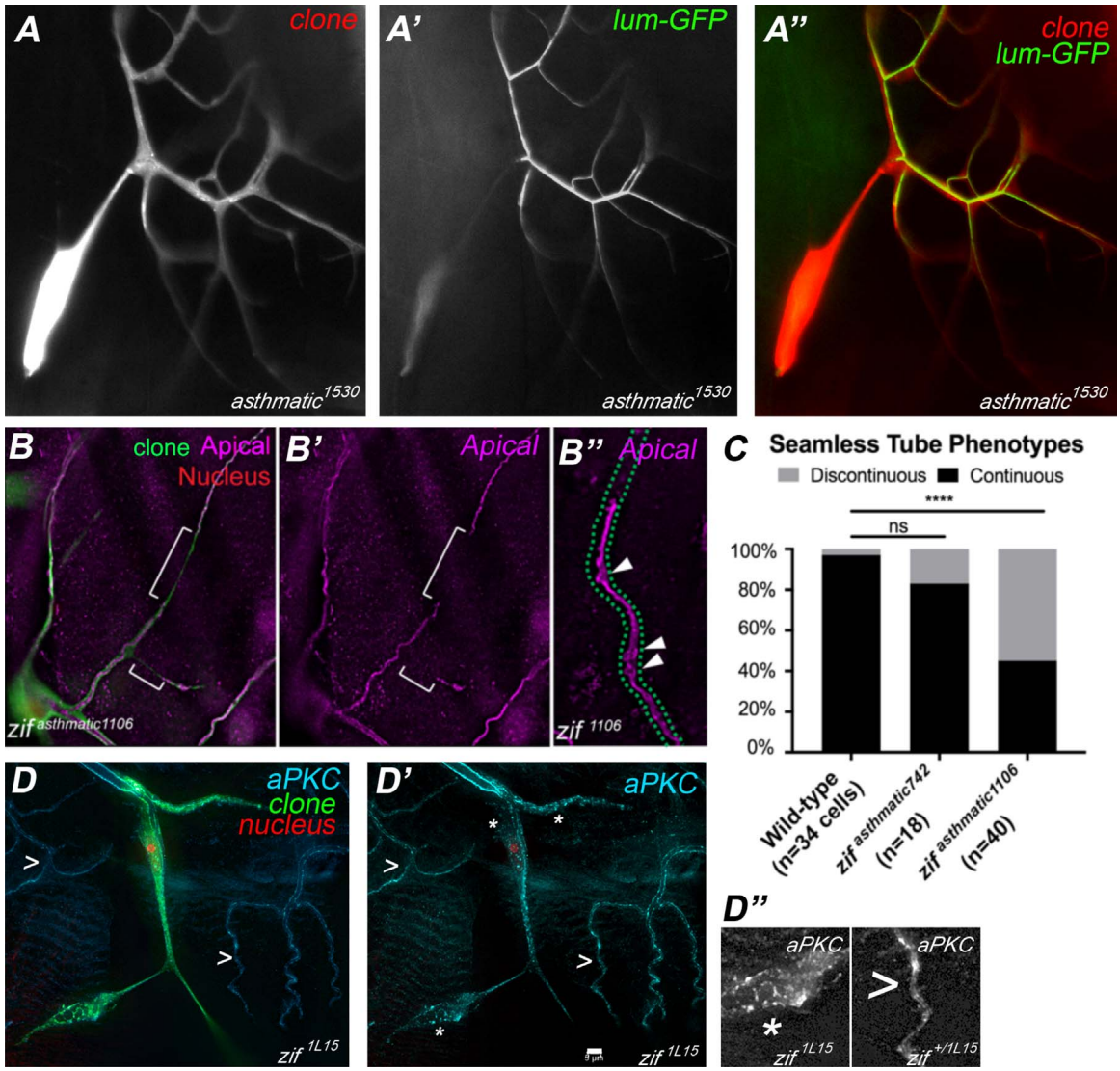

Fig. 7. Mutations in *zif* disrupt maintenance of apical polarity in seamless tubes. Terminal cells mutant for *asthmatic* (A, red in A") lack gas-filled tubes; however, they do make tubes that lack gas-filling, as revealed by the localization of a secreted GFP – lum-GFP – in the lumenal space (A', green in A"). Mapping studies revealed that *asthmatic*^{1530} (shown in A-A") is not part of the same complementation group as *asthmatic*^{742} and ^{1106}, which we now identify as new alleles of *zif*. We will henceforth refer to only *1530* as *asthmatic* and rename the *742* and *1106* as alleles of *zif*. Staining of apical membranes in *zif*^{1106} terminal cells (B-B"), reveals the presence of tube shape irregularities (arrowheads in B") and discontinuities (indicated by [in B and B'). Discontinuity defects were quantified in (C). To determine the null phenotype, we examined *zif*^{1L15} mutant terminal cells (green, D). We found that seamless tubes were largely absent or were severely truncated and that apical membrane antigens such as aPKC (cyan) and Wkdpep (not shown) were no longer enriched on the lumenal membrane, but were dispersed throughout the cell (D and D'). The location of the terminal cell nucleus is revealed by expression of DsRED2nls (red, D). Note that apical membrane localization of aPKC in neighboring heterozygous terminal cells is intact (> in D, D'). In D" adjacent sections of the panel in D' are shown enlarged (*, portion of *zif* clone, > portion of *zif*$^{+/-}$ control cell). Scale Bar (D') = 5 μm, applies to A-D'.

the tracheal system did not affect localization of aPKC (data not shown). In the absence of a proper apical domain, terminal cell growth and branching appear compromised with subsequent induction of compensatory branching in the adjacent stalk cell.

Interestingly, the three complementation groups we chose to further characterize all impacted related growth pathways, with *sprout* and *denuded* acting upstream and downstream, respectively, of the TOR pathway, and *zif* showing apical polarity maintenance defects similar to those we reported with loss of TOR pathway signaling, raising the possibility that Zif may also factor into Tor signaling. Future studies examining the epistatic relationship between Zif and Tor (or Hippo) will establish if these genes are acting with a single pathway or are acting in parallel but converging on an overlapping set of downstream targets. Going forward, it will be important to understand how the FGF pathway, which drives all tracheal branching events, intersects with the Hippo and Tor cell growth pathways. In particular, it will be very interesting to see how, or if, local activation of the FGFR pathway in tracheal terminal cells provokes a growth and branching response that differs from the global activation of the FGFR pathway, or the global de-repression of Tor or Hippo pathways. All of the latter result in the induction of ectopic seamless tubes around the terminal cell nucleus, whereas a response to FGF point sources (hypoxia-induced branchless expression) is thought to sculpt the unique shapes (branching pattern) of each terminal cell without eliciting ectopic seamless tube growth in the soma.

Acknowledgements

ASB would like to acknowledge funding from the Taub Institute. JR would like to acknowledge funding from NIH pre-doctoral fellowship (F31 HL 132501). ASG would like to acknowledge funding from NIH 2R01GM089782 and the Dean's office at Columbia University Medical Center.

References

Bacon, N.C., Wappner, P., O'Rourke, J.F., Bartlett, S.M., Shilo, B., Pugh, C.W., Ratcliffe, P.J., 1998. Regulation of the Drosophila bHLH-PAS protein Sima by hypoxia: functional evidence for homology with mammalian HIF-1 alpha. Biochem. Biophys. Res. Commun. 249, 811–816.

Baudier, J., 2018. ATAD3 proteins: brokers of a mitochondria-endoplasmic reticulum connection in mammalian cells. Biol. Rev. Camb. Philos. Soc. 93, 827–844.

Bayarmagnai, B., Nicolay, B.N., Islam, A.B., Lopez-Bigas, N., Frolov, M.V., 2012. Drosophila GAGA factor is required for full activation of the dE2f1-Yki/Sd transcriptional program. Cell Cycle 11, 4191–4202.

Centanin, L., Dekanty, A., Romero, N., Irisarri, M., Gorr, T.A., Wappner, P., 2008. Cell autonomy of HIF effects in Drosophila: tracheal cells sense hypoxia and induce terminal branch sprouting. Dev. Cell 14, 547–558.

Chang, K.C., Garcia-Alvarez, G., Somers, G., Sousa-Nunes, R., Rossi, F., Lee, Y.Y., Soon, S.B., Gonzalez, C., Chia, W., Wang, H., 2010. Interplay between the transcription factor Zif and aPKC regulates neuroblast polarity and self-renewal. Dev. Cell 19, 778–785.

Dekanty, A., Lavista-Llanos, S., Irisarri, M., Oldham, S., Wappner, P., 2005. The insulin-PI3K/TOR pathway induces a HIF-dependent transcriptional response in Drosophila by promoting nuclear localization of HIF-alpha/Sima. J. Cell Sci. 118, 5431–5441.

Duronio, R.J., O'Farrell, P.H., 1995. Developmental control of the G1 to S transition in Drosophila: cyclin Eis a limiting downstream target of E2F. Genes Dev. 9, 1456–1468.

Duronio, R.J., O'Farrell, P.H., Xie, J.E., Brook, A., Dyson, N., 1995. The transcription factor E2F is required for S phase during Drosophila embryogenesis. Genes Dev. 9, 1445–1455.

Edgar, B.A., 2006. How flies get their size: genetics meets physiology. Nat. Rev. Genet. 7, 907–916.

Fernandez-Almonacid, R., Rosen, O.M., 1987. Structure and ligand specificity of the Drosophila melanogaster insulin receptor. Mol. Cell Biol. 7, 2718–2727.

Francis, D., Ghabrial, A.S., 2015. Compensatory branching morphogenesis of stalk cells in the Drosophila trachea. Development 142, 2048–2057.

Ghabrial, A.S., Levi, B.P., Krasnow, M.A., 2011. A systematic screen for tube morphogenesis and branching genes in the Drosophila tracheal system. PLoS Genet. 7, e1002087.

Guertin, D.A., Guntur, K.V., Bell, G.W., Thoreen, C.C., Sabatini, D.M., 2006. Functional genomics identifies TOR-regulated genes that control growth and division. Curr. Biol. 16, 958–970.

Guha, A., Kornberg, T.B., 2005. Tracheal branch repopulation precedes induction of the Drosophila dorsal air sac primordium. Dev. Biol. 287, 192–200.

Guillemin, K., Groppe, J., Ducker, K., Treisman, R., Hafen, E., Affolter, M., Krasnow, M.A., 1996. The pruned gene encodes the Drosophila serum response factor and regulates cytoplasmic outgrowth during terminal branching of the tracheal system. Development 122, 1353–1362.

Harel, T., Yoon, W.H., Garone, C., Gu, S., Coban-Akdemir, Z., Eldomery, M.K., Posey, J.E., Jhangiani, S.N., Rosenfeld, J.A., Cho, M.T., Fox, S., Withers, M., Brooks, S.M., Chiang, T., Duraine, L., Erdin, S., Yuan, B., Shao, Y., Moussallem, E., Lamperti, C., Donati, M.A., Smith, J.D., McLaughlin, H.M., Eng, C.M., Walkiewicz, M., Xia, F., Pippucci, T., Magini, P., Seri, M., Zeviani, M., Hirano, M., Hunter, J.V., Srour, M., Zanigni, S., Lewis, R.A., Muzny, D.M., Lotze, T.E., Boerwinkle, E., Baylor-Hopkins Center for Mendelian, G., University of Washington Center for Mendelian, G., Gibbs, R.A., Hickey, S.E., Graham, B.H., Yang, Y., Buhas, D., Martin, D.M., Potocki, L., Graziano, C., Bellen, H.J., Lupski, J.R., 2016. Recurrent de novo and biallelic variation of ATAD3A, encoding a mitochondrial membrane protein, results in distinct neurological syndromes. Am. J. Hum. Genet. 99, 831–845.

Hietakangas, V., Cohen, S.M., 2009. Regulation of tissue growth through nutrient sensing. Annu. Rev. Genet. 43, 389–410.

Jarecki, J., Johnson, E., Krasnow, M.A., 1999. Oxygen regulation of airway branching in Drosophila is mediated by branchless FGF. Cell 99, 211–220.

JayaNandanan, N., Mathew, R., Leptin, M., 2014. Guidance of subcellular tubulogenesis by actin under the control of a synaptotagmin-like protein and Moesin. Nat. Commun. 5, 3036.

Jiang, N., Soba, P., Parker, E., Kim, C.C., Parrish, J.Z., 2014. The microRNA bantam regulates a developmental transition in epithelial cells that restricts sensory dendrite growth. Development 141, 2657–2668.

Johnson, R., Halder, G., 2014. The two faces of Hippo: targeting the Hippo pathway for regenerative medicine and cancer treatment. Nat. Rev. Drug Discov. 13, 63–79.

Lee, T., Hacohen, N., Krasnow, M., Montell, D.J., 1996. Regulated Breathless receptor tyrosine kinase activity required to pattern cell migration and branching in the Drosophila tracheal system. Genes Dev. 10, 2912–2921.

Orr-Weaver, T.L., 2015. When bigger is better: the role of polyploidy in organogenesis. Trends Genet. 31, 307–315.

Pierce, S.B., Yost, C., Britton, J.S., Loo, L.W., Flynn, E.M., Edgar, B.A., Eisenman, R.N., 2004. dMyc is required for larval growth and endoreplication in Drosophila. Development 131, 2317–2327.

Reddy, B.V., Rauskolb, C., Irvine, K.D., 2010. Influence of fat-hippo and notch signaling on the proliferation and differentiation of Drosophila optic neuroepithelia. Development 137, 2397–2408.

Schottenfeld-Roames, J., Ghabrial, A.S., 2012. Whacked and Rab35 polarize dynein-motor-complex-dependent seamless tube growth. Nat. Cell Biol. 14, 386–393.

Schottenfeld-Roames, J., Rosa, J.B., Ghabrial, A.S., 2014. Seamless tube shape is constrained by endocytosis-dependent regulation of active Moesin. Curr. Biol. 24, 1756–1764.

Tumaneng, K., Russell, R.C., Guan, K.L., 2012a. Organ size control by Hippo and TOR pathways. Curr. Biol. 22, R368–R379.

Tumaneng, K., Schlegelmilch, K., Russell, R.C., Yimlamai, D., Basnet, H., Mahadevan, N., Fitamant, J., Bardeesy, N., Camargo, F.D., Guan, K.L., 2012b. YAP mediates crosstalk between the Hippo and PI(3)K-TOR pathways by suppressing PTEN via miR-29. Nat. Cell Biol. 14, 1322–1329.

Weaver, M., Krasnow, M.A., 2008. Dual origin of tissue-specific progenitor cells in Drosophila tracheal remodeling. Science 321, 1496–1499.

Zhang, H., Stallock, J.P., Ng, J.C., Reinhard, C., Neufeld, T.P., 2000. Regulation of cellular growth by the Drosophila target of rapamycin dTOR. Genes Dev. 14, 2712–2724.

Zhang, P., Pei, C., Wang, X., Xiang, J., Sun, B.F., Cheng, Y., Qi, X., Marchetti, M., Xu, J.W., Sun, Y.P., Edgar, B.A., Yuan, Z., 2017. A balance of Yki/Sd activator and E2F1/Sd repressor complexes controls cell survival and affects organ size. Dev. Cell 43 (603–617), e605.

Zhou, F., Qiang, K.M., Beckingham, K.M., 2016. Failure to burrow and tunnel reveals roles for jim lovell in the growth and endoreplication of the Drosophila larval tracheae. PLoS One 11, e0160233.

Zielke, N., Kim, K.J., Tran, V., Shibutani, S.T., Bravo, M.J., Nagarajan, S., van Straaten, M., Woods, B., von Dassow, G., Rottig, C., Lehner, C.F., Grewal, S.S., Duronio, R.J., Edgar, B.A., 2011. Control of Drosophila endocycles by E2F and CRL4(CDT2). Nature 480, 123–127.